

# Low temperature synthesis of AlN by addition of various Li-salts

Yoshikazu Kameshima\*, Masaki Irie<sup>1</sup>, Atsuo Yasumori<sup>2</sup>, Kiyoshi Okada

*Department of Metallurgy and Ceramics Science, Tokyo Institute of Technology, O-okayama, Meguro, Tokyo 152-8552, Japan*

Received 7 November 2003; received in revised form 19 December 2003; accepted 27 December 2003

Available online 6 May 2004

## Abstract

The effect of various Li-salts on the low temperature synthesis of AlN by direct nitridation of Al metal was investigated using four Al powders with average particle sizes of 3, 20, 100 and 150  $\mu\text{m}$ . These were mixed with various Li-salts ( $\text{LiNO}_3$ ,  $\text{LiOH}\cdot\text{H}_2\text{O}$  and  $\text{Li}_2\text{CO}_3$ ) in different concentrations and fired at various temperatures under flowing  $\text{N}_2$ . The as-received Al powders without Li addition showed AlN formation at about 600 °C in the 3 and 20  $\mu\text{m}$  samples but no AlN formation up to 850 °C in the 100 and 150  $\mu\text{m}$  samples. The crystallinity of the AlN products, where formed, was however low. By contrast, all the Al powders with added Li-salts showed AlN formation up to 800 °C, with  $\text{LiOH}\cdot\text{H}_2\text{O}$  being especially effective. Thus, the AlN formation temperature can be significantly lowered in the coarser powders by the addition of Li-salts but the effect is less in the finer powders which undergo low temperature nitridation below the melting point of Al metal even without Li. The crystallinity of the AlN products was higher in the samples containing Li-salts than without Li-salts.

© 2004 Elsevier Ltd. All rights reserved.

**Keywords:** AlN; Nitridation; Phase development; Crystallization; Al

## 1. Introduction

AlN has very good thermal conductivity, high electrical resistivity and similar thermal expansion coefficient to Si.<sup>1</sup> These properties make AlN attractive for IC substrates and packaging materials, while its high thermal conductivity permits a higher component density and increased opportunity for down-sizing of electronic circuits. The replacement of conventional alumina substrates by AlN ceramics is thus increasing.

For AlN powder, three major preparation methods are available: (1) carbothermal, (2) direct nitridation and (3) gas phase synthesis. Carbothermal synthesis is the most commonly used method for AlN powder production. In this method, AlN is formed by reduction of  $\text{Al}_2\text{O}_3$  or  $\text{Al}(\text{OH})_3$  with carbon powder at high temperatures. Although high performance products with high purity and uniform particle size can be obtained by the carbothermal method,<sup>2</sup> the

synthesis temperatures are usually around 1700–1900 °C and should preferably be lowered. Another important synthesis method for AlN production is the direct nitridation of Al metal with  $\text{N}_2$  or  $\text{NH}_3$  at high temperatures.<sup>3</sup> Since the reaction is exothermic, the process is somewhat difficult to control and the AlN product is highly aggregated, making it necessary to crush it after synthesis. However, direct nitridation has the advantage of being a simpler synthesis than the carbothermal method and provides more variety in the powder properties of the product. The third synthetic method is nitridation by gas phase reaction using such as alkyl-Al compounds.<sup>4</sup> This method produces very fine high-purity particles but has the disadvantages of producing a product with lower oxidation resistance and requires more expensive starting materials.

Of these three methods, the possibility of lowering the AlN synthesis temperature is greatest for direct nitridation because of the very low melting temperature of Al metal (660.2 °C) which is used for the nitridation. The lowering of the AlN synthesis temperature in direct nitridation has been investigated by (1) alloying the Al metal, (2) reacting under  $\text{N}_2$  and  $\text{NH}_3$  atmospheres at high pressure and (3) mechanochemical grinding. Komeya et al.<sup>5</sup> used Al–Li, Al–Y and Al–Ca alloys as starting materials and succeeded in lowering the nitridation temperature to about 800 °C in

\* Corresponding author. Tel.: +81-3-5734-2525; fax: +81-3-5734-3355.

E-mail address: [ykameshi@ceram.titech.ac.jp](mailto:ykameshi@ceram.titech.ac.jp) (Y. Kameshima).

<sup>1</sup> Present address: Toshiba Ceramics Co., Soya, Hatano, Kanagawa 257-8566, Japan.

<sup>2</sup> Present address: Department of Materials Engineering, Tokyo Science University, Yamazaki, Noda, Chiba 278-8510, Japan

the case of the Al–Li 2.3 mass% alloy. They proposed that the low temperature formation mechanism involves the enhancement of N<sub>2</sub> diffusion by a Li–Al–O phase formed during heating of the Al–Li alloy. Synthesis under a pressurized N<sub>2</sub> atmosphere is also effective in lowering the AlN synthesis temperature. Okada et al.<sup>6</sup> demonstrated the formation of AlN monoliths by heating green bodies of Al powder at about 600 °C under 1.4 MPa N<sub>2</sub> pressure. Mechanochemical AlN synthesis by the direct nitridation method was investigated by Calka and Nikolov<sup>7</sup> and Nikolov et al.<sup>8</sup> They succeeded in forming AlN at about 1000 °C by reacting mechanochemically treated Al powder under ambient N<sub>2</sub> pressure, this temperature being further lowered to about 700 °C by heating the powder under 0.6 MPa of NH<sub>3</sub>. However, synthesis at high pressure requires a high-pressure vessel and is not suitable for industrial production because of the increased cost. These experimental results suggest that it would be interesting to examine in more detail the effectiveness of Li additions using various Li-salts rather than alloying the Al metal with Li. Such Li additions should form an Li–Al–O phase more readily than the Al–Li alloys reported by Komeya et al.<sup>5</sup>, suggesting the possibility of a considerable lowering temperature of the AlN synthesis.

In this paper, the effect of additions of various Li-salts on the low temperature synthesis of AlN by direct nitridation of Al powder was investigated, using four Al powders with different particle sizes.

## 2. Experimental

### 2.1. Sample preparation

Four Al powders, with average particle sizes from 3 to 150 μm, were used as the starting materials. The Li-salts were LiNO<sub>3</sub>, LiOH·H<sub>2</sub>O and Li<sub>2</sub>CO<sub>3</sub> (Wako Chemicals, Tokyo, Japan). The Al powders and Li-salts were gently mixed, using an agate mortar and pestle for 15 min, to avoid adhesion of the Al particles by the mixing. The ratios of Li-salts in the mixtures ranged from 0.1 to 5.0 mass% Li expressed as Li/(Li + Al). The mixed powder (0.15 g) was heated in a tube furnace in flowing dry N<sub>2</sub> (1 l/min), carefully purging the system with N<sub>2</sub> before starting the heating. The samples were heated at 5 °C/min from room temperature to 200 °C below the soaking temperature, which was approached at a rate of 1 °C/min to avoid overshooting. The soaking time at temperature was 1–8 h and the cooling rate was 5 °C/min.

### 2.2. Characterization

Thermal analysis of the samples was performed using a DTA–TG instrument (Thermoplus TG8120, Rigaku, Tokyo, Japan). The amount of sample was about 10 mg and the heating rate was 10 °C/min in flowing N<sub>2</sub>. Nitridation of the

samples was calculated from the recorded thermo gravimetric weight change using the following equation:

$$\text{Conversion ratio (\%)} = \frac{M_{\text{AlN}} \times m_{\text{TP}}}{M_{\text{N}} \times m_{\text{Al}}} \times 100$$

where  $M_{\text{AlN}}$  and  $M_{\text{N}}$  are the molecular weights of AlN and N, and  $m_{\text{Al}}$  and  $m_{\text{TP}}$  are the sample weights before and after the heating. The crystalline phases in the samples were examined by X-ray diffractometer (XRD; LabX XRD-6100, Shimadzu, Kyoto, Japan) using monochromated Cu K $\alpha$  radiation. The crystallite size ( $D$ ) and lattice strain ( $\eta$ ) of the as-received Al samples was calculated from the Hall equation:

$$\beta \cos \theta = \frac{\lambda}{D} + 2\eta \sin \theta$$

where  $\beta$  is the integral width of reflection,  $\theta$  is the Bragg angle,  $\lambda$  is the X-ray wavelength and  $\eta$  is the lattice strain. However, the crystallite size of AlN had to be calculated by the Scherrer equation using the integral width of the (1 0 0) reflection because of the limitation in the number of reflections for the Hall plot. The surface chemical compositions of the samples were investigated using X-ray photoelectron spectroscopy (XPS; model 5500MT, Perkin-Elmer, Physical Electronics, Minnesota, USA). The XPS measurements were performed using monochromated Al K $\alpha$  radiation at an instrument pressure of <math>10^{-9}</math> Torr and the binding energy was referenced to the C 1s of adventitious hydrocarbon at 284.6 eV. The thickness of surface oxide phase of the Al powders was evaluated by the calculation method reported by Okada et al.<sup>9</sup> The microstructures of the samples were observed by scanning electron microscope (SEM; JSM-5310, JEOL, Tokyo, Japan) at an accelerating voltage of 20 kV.

## 3. Results and discussion

### 3.1. Al powder

The properties of the four reactant Al powders are listed in Table 1. The average particle sizes were 3, 20, 100 and 150 μm. The particle shape of these powders was irregular, and the crystallite sizes calculated from the Hall method ranged from 62 to 71 nm, showing less variation than their

Table 1  
Properties of the Al starting powders

	Sample Al			
	3 μm	20 μm	100 μm	150 μm
Purity (mass%)	99.9	99.9	99.99	99.5
Particle size (μm)	3	20	100	150
Crystallite size (nm)	68	71	62	66
Lattice strain (%)	0.12	–	–	–
Surface oxide thickness (nm)	3.5	3.6	2.9	3.3
Supplier	Soekawa	Soekawa	Soekawa	Wako

Table 2  
Properties of Li-salts

	Li-salt				
	LiNO <sub>3</sub>	LiOH·H <sub>2</sub> O	Li <sub>2</sub> CO <sub>3</sub>	LiCl	LiF
Melting temperature (°C)	261	450–471	723	606	842
Boiling temperature (°C)	–	–	–	1382	1676
Decomposition temperature (°C)	600	924	1310	–	–
Hygroscopy	Yes	No	No	Yes	No

particle sizes. The Hall plots show that all the powders except the 3  $\mu\text{m}$  sample have negligibly small lattice strain, due to the high malleability of Al metal. The lattice strain observed in the 3  $\mu\text{m}$  sample may have been introduced by the mechanical reduction of the particle size. The thickness of the surface oxide layers evaluated from XPS analysis ranged from 2.9 to 3.6 nm and was almost the same for all the samples.

### 3.2. Effect of Li-salt

The effect of Li additions on the temperature of AlN synthesis was investigated by using various Li-salts to identify the best additive. Some of the properties required by the additives are listed in Table 2 for the compounds LiNO<sub>3</sub>, LiOH·H<sub>2</sub>O, Li<sub>2</sub>CO<sub>3</sub>, LiCl and LiF. The important properties of an additive are a low melting temperature (preferably lower than that of Al metal (660.2 °C)) and anions which can be thermally removed during AlN synthesis. On the basis of these two criteria, LiNO<sub>3</sub>, LiOH·H<sub>2</sub>O and Li<sub>2</sub>CO<sub>3</sub> were selected as candidates.

Three Li-containing samples were prepared by mixing the three selected Li-salts (0.5 mass% Li) with the 20  $\mu\text{m}$  powder. Fig. 1 shows the AlN conversion curves of the three Li-containing Al samples as a function of heating temperature. The conversion temperatures were 620, 640 and 645 °C in the samples containing LiOH·H<sub>2</sub>O, LiNO<sub>3</sub> and Li<sub>2</sub>CO<sub>3</sub>,

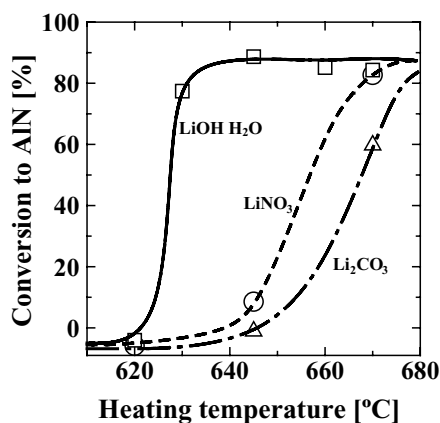


Fig. 1. AlN conversion curves of samples containing LiNO<sub>3</sub>, LiOH·H<sub>2</sub>O and Li<sub>2</sub>CO<sub>3</sub> (0.5 mass% Li) as a function of heating temperature.

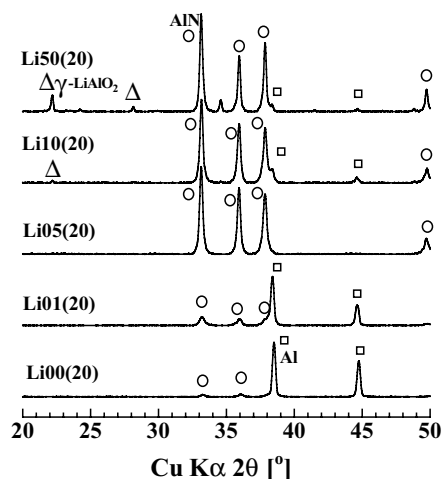


Fig. 2. XRD patterns of Al samples (20  $\mu\text{m}$ ) containing various amounts of LiOH·H<sub>2</sub>O, heated at 775 °C for 8 h.

respectively. The AlN conversion rate of the sample containing LiOH·H<sub>2</sub>O was steeper than those containing LiNO<sub>3</sub> and Li<sub>2</sub>CO<sub>3</sub>. The maximum conversion ratio was about 90% at 645 °C in the sample containing LiOH·H<sub>2</sub>O. These results indicate that the most effective additive for lowering the AlN formation temperature is LiOH·H<sub>2</sub>O.

### 3.3. Effect of the amount of LiOH·H<sub>2</sub>O

In order to determine the optimum amount of Li to be added, samples of the 20  $\mu\text{m}$  Al powder were mixed with LiOH·H<sub>2</sub>O in concentrations of 0.1, 0.5, 1.0 and 5.0 mass% Li. The XRD patterns of these samples heated at 775 °C for 8 h are shown in Fig. 2. In samples containing up to 0.1 mass% Li, the principal phase is Al with only a small amount of AlN formed. In contrast, the XRD pattern of the sample containing 0.5 mass% Li is very different, containing all the peaks of AlN and no Al peaks. With further increase of Li up to 1.0 mass%, small peaks of Al metal are present, together with a pattern identified as  $\gamma$ -LiAlO<sub>2</sub>. The intensities of the  $\gamma$ -LiAlO<sub>2</sub> peaks become stronger with increasing Li content up to 5.0 mass%. The AlN conversion ratios of these samples are shown as a function of Li content in Fig. 3. The Li addition is found to be very effective in enhancing AlN formation in concentrations up to 0.5 mass%, the maximum conversion being >90 mass% in the 0.5 mass% Li-containing sample. However, excess Li addition above 0.5 mass% causes a slight decrease of the AlN conversion ratio. Thus, the optimum amount of Li-addition is 0.5 mass%.

### 3.4. Effect of the Al particle size

The effect of the Al particle size in Li-assisted AlN synthesis was examined using the four Al powders with particle sizes ranging from 3 to 150  $\mu\text{m}$ . The AlN conversion curves of the as-received and 0.5 mass% Li-containing samples are compared in these four Al powders in Fig. 4a–d, respectively. In the 3 and 20  $\mu\text{m}$  samples, the AlN conversion curves do

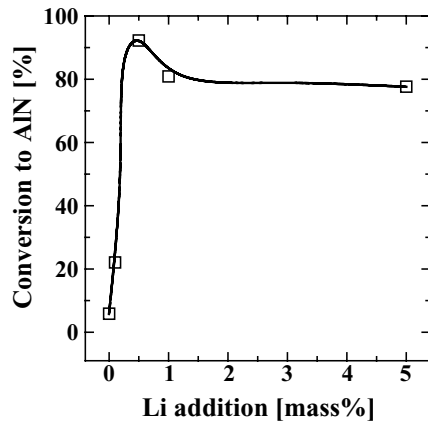


Fig. 3. Change of AlN conversion ratios in the 20  $\mu\text{m}$  samples heated at 775  $^{\circ}\text{C}$  for 8 h as a function of Li addition.

not differ significantly by the addition of Li, with even a slightly higher starting temperature for AlN conversion being recorded for the 20  $\mu\text{m}$  Li-containing sample. Since Al powder, especially fine powder, adheres readily, increasing the particle size during mixing, these Li-containing samples are thought to have undergone an apparent increase in their particle size during the mixing with LiOH·H<sub>2</sub>O even though

this was carried out gently by mortar and pestle for a short time. These increases in the particle sizes are thought to be responsible for their poor degree of AlN conversion even in the presence of Li. This negative effect is observed in Fig. 1 because the 20  $\mu\text{m}$  Li00(20) sample without added Li but similarly mixed by mortar and pestle shows only a small amount of AlN even when heated at 775  $^{\circ}\text{C}$  for 8 h.

By contrast, Li additions to the coarser 100 and 150  $\mu\text{m}$  powders produce very much lowered AlN conversion temperatures. The Li-free control samples show no AlN conversion even when heated to 825  $^{\circ}\text{C}$  whereas the Li-containing samples clearly show a lowering of the AlN conversion temperature. The starting temperatures of AlN formation in the Li-containing 100 and 150  $\mu\text{m}$  samples are about 600 and 750  $^{\circ}\text{C}$ , respectively. Thus, the addition of a small amount of LiOH·H<sub>2</sub>O is especially effective in lowering the AlN synthesis temperature in coarser Al powders. AlN synthesis is therefore concluded to be possible below 800  $^{\circ}\text{C}$  by addition of Li even in coarse Al powders.

### 3.5. Characterization

To examine the effect of Li addition on low temperature AlN formation, the thermal behavior of the 20  $\mu\text{m}$

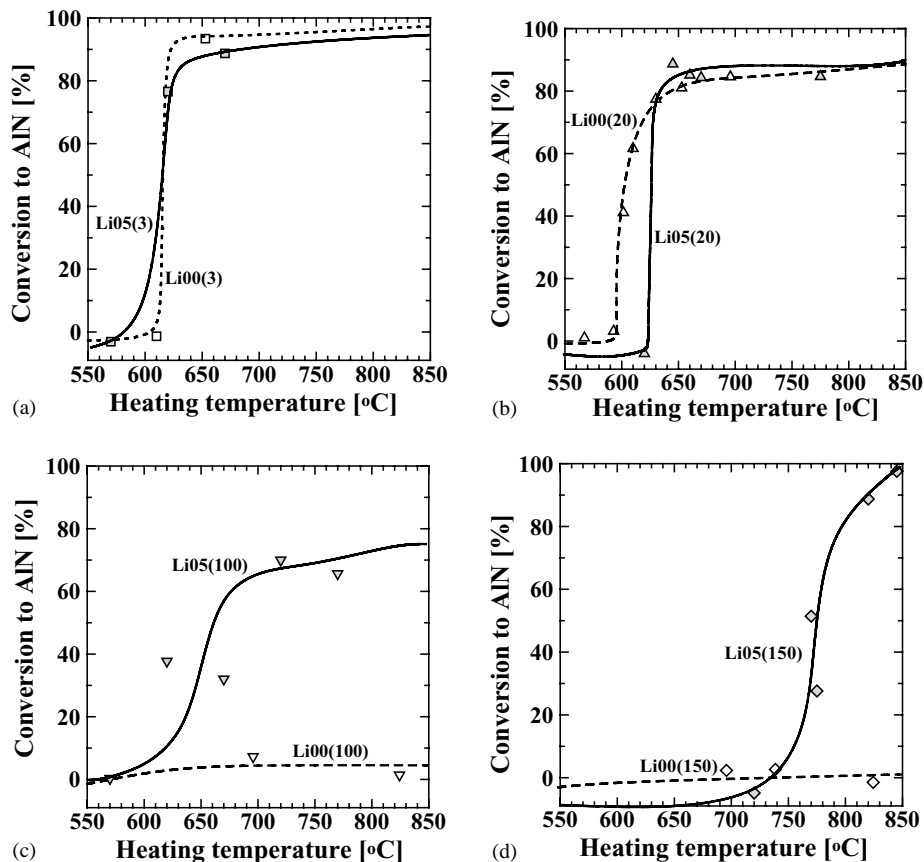


Fig. 4. AlN conversion curves in as-received (Li00) and 0.5 mass% Li-containing samples (Li05) as a function of heating temperature: (a) 3  $\mu\text{m}$  sample, (b) 20  $\mu\text{m}$  sample, (c) 100  $\mu\text{m}$  sample, and (d) 150  $\mu\text{m}$  sample.

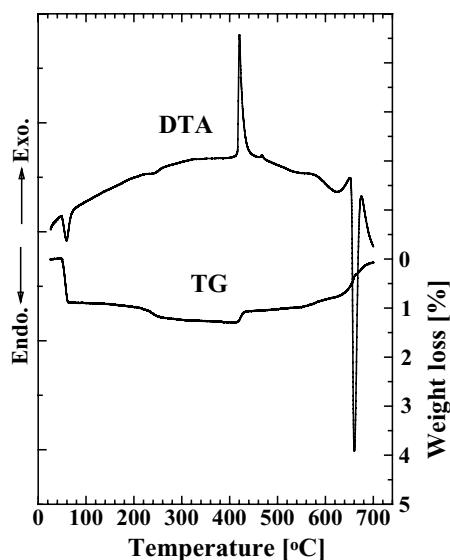


Fig. 5. DTA and TG curves of 0.5 mass% Li-containing 20  $\mu\text{m}$  sample (Li05(20)).

sample was analyzed by DTA and TG (Fig. 5). The DTA curve shows clear endothermic peaks at 60 and 660  $^{\circ}\text{C}$ , attributed to the dehydration of  $\text{LiOH}\cdot\text{H}_2\text{O}$  and melting of Al, respectively. The observed weight loss at 60  $^{\circ}\text{C}$  is 0.9 mass%, smaller than the calculated weight loss for the dehydration of  $\text{LiOH}\cdot\text{H}_2\text{O}$  to LiOH (1.26 mass%). A weak endothermic peak was also observed at 240  $^{\circ}\text{C}$  with an associated weight loss of about 0.2–0.3 mass%. Although the reason for this endothermic reaction is not clear, the combined weight loss at 60 and 240  $^{\circ}\text{C}$  is close to the calculated weight loss for dehydration of  $\text{LiOH}\cdot\text{H}_2\text{O}$ . One other strong and one weak exothermic peak was observed at 420 and 468  $^{\circ}\text{C}$ , respectively. The former is attributed to crystallization of  $\gamma\text{-LiAlO}_2$  but the reason for the latter peak is not clear. The crystallization reaction is associated with a weight gain of about 0.25 mass%, thought to be due to oxidation of Al during  $\gamma\text{-LiAlO}_2$  formation. The TG curve shows a gradual weight gain above the crystallization temperature, attributed to nitridation of Al to AlN. DTA–TG analysis therefore shows that the formation of  $\gamma\text{-LiAlO}_2$  occurs on the surfaces of the Al powders preceding AlN formation in the Li-containing sample. As suggested by Komeya et al.<sup>5</sup>, this phase accelerates diffusion of  $\text{N}_2$  in Al powder and plays an important role in lowering the AlN conversion temperature.

The crystallinity of the resulting AlN was evaluated from the crystallite size measurements. Changes in the crystallite sizes of the as-received and Li-containing (0.5 mass%) samples (20  $\mu\text{m}$ ) are shown in Fig. 6 as a function of heating temperature. The crystallite sizes of the AlN from the as-received samples range from 12 to 14 nm while those from the Li-containing samples range from 17 to 31 nm. The crystallite sizes of the AlN from the Li-containing samples are larger than those from the as-received samples and the

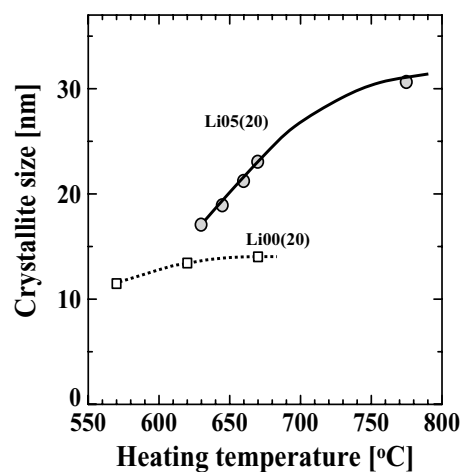


Fig. 6. Changes of crystallite sizes of AlN products in as-received (Li00(20)) and 0.5 mass% Li-containing (Li05(20)) 20  $\mu\text{m}$  samples as a function of heating temperature.

increased growth of crystallite size with higher heating temperature is larger in the Li-containing samples. Thus, the addition of Li is not only effective for lowering the AlN formation temperature but also for enhancing the crystallinity of the resulting AlN.

#### 4. Conclusion

The effect of Li additions on the low temperature synthesis of AlN by direct nitridation was investigated using  $\text{LiNO}_3$ ,  $\text{LiOH}\cdot\text{H}_2\text{O}$  and  $\text{Li}_2\text{CO}_3$  in conjunction with four Al powders ranging in particle size from 3 to 150  $\mu\text{m}$ . The following results were obtained:

- (1) Of the three Li-salts examined ( $\text{LiNO}_3$ ,  $\text{LiOH}\cdot\text{H}_2\text{O}$  and  $\text{Li}_2\text{CO}_3$ ),  $\text{LiOH}\cdot\text{H}_2\text{O}$  was the most effective for lowering of the AlN synthesis temperature.
- (2) Li additions were less effective in lowering the AlN synthesis temperature in the finer Al powders (3 and 20  $\mu\text{m}$ ) but were very effective with the coarser Al powders (100 and 150  $\mu\text{m}$ ).
- (3) Since the added  $\text{LiOH}\cdot\text{H}_2\text{O}$  was found to form  $\gamma\text{-LiAlO}_2$  on heating at about 420  $^{\circ}\text{C}$ , this phase is thought to play an important role in enhancing  $\text{N}_2$  diffusion to form AlN at low temperature.
- (4) Li addition was also effective in producing an AlN product of higher crystallinity.

#### Acknowledgements

We are grateful to Professor K.J.D. MacKenzie of Victoria University of Wellington for critical reading and editing of the manuscript.

## References

1. Tsuge, A. and Shinozaki, K., *Ceramics Substrates for Functional Circuits*. Ohm, Tokyo, 1984, pp. 57–75.
2. Selvasurary, G. and Sheet, L., Aluminium nitride: review of synthesis methods. *Mater. Sci. Technol.* 1993, **9**, 463–473.
3. Weimer, A. W., Cochran, G. A., Eisman, G. A., Henley, J. P., Hook, B. D. and Mills, L. K., Rapid Process for manufacturing aluminum nitride powder. *J. Am. Ceram. Soc.* 1994, **77**, 3–18.
4. Nagano, U., Features of aluminum nitride and its applications. *Seramikkusu* 2001, **36**, 262–264.
5. Komeya, K., Matsukaze, N. and Meguro, T., Synthesis of AlN by direct nitridation of Al alloys. *J. Ceram. Soc. Jpn.* 1993, **101**, 1319–1323.
6. Okada, T., Obata, M., Toriyama, M. and Kanzaki, S., Direct nitridation of aluminum compacts in low temperature and pressured N<sub>2</sub> atmosphere. *J. Ceram. Soc. Jpn.* 1999, **107**, 455–459.
7. Calka, A. and Nikolov, J. I., Direct synthesis of AlN and Al–AlN composites by room temperature magneto ball milling: the effect of milling condition on formation of nanostructures. *Nano Struct. Mater.* 1995, **6**, 409–412.
8. Nikolov, J. I., Williams, J. S., Llewellyn, D. J. and Calka, A., Phase evolution during ball milling of AlN in NH<sub>3</sub> and subsequent annealing. *Mater. Res. Soc. Symp. Proc.* 1998, **481**, 649–654.
9. Okada, K., Fukuyama, K. and Kameshima, Y., Characterization of surface-oxidized phase in silicon nitride and silicon oxynitride powders by X-ray photoelectron spectroscopy. *J. Am. Ceram. Soc.* 1995, **78**, 2021–2026.